JOURNAL OF COMPUTATIONAL BIOLOGY
Volume 26, Number 0, 2019
© Mary Ann Liebert, Inc.
Pp. 1–12
DOI: 10.1089/cmb.2019.0052

Research Article

Curcumin-Synthetic Analogs Library Screening by Docking and Quantitative Structure–Activity Relationship Studies for AXL Tyrosine Kinase Inhibition in Cancers

FATIMA GHRIFI, LOUBNA ALLAM, LAKHLILI WIAME, and AZEDDINE IBRAHIMI

Downloaded by STOCKHOLMS UNIVERSITET from www.liebertpub.com at 04/25/19. For personal use only.

ABSTRACT

AXL is an important drug target for cancers. Two-dimensional quantitative structure–activity relationship (2D-QSAR) tests were performed to elucidate a relationship between molecular structures and the activity of a series of 400 curcumin derivatives subjected to AXL kinase by ATP competition in the catalytic site. The partial least square regression method implanted in molecular operating environment software was applied to develop QSAR models, which were further validated for statistical significance by internal and external validation. The best model has proven to be statistically robust with a good predictive correlation of $R^2 = 0.996$ and a significant cross-validation correlation coefficient of $q^2 = 0.707$. Docking analysis reveled that three curcumin derivatives have the best affinity for AXL and formed a hydrogen bond with the important amino acid residues in the binding pocket. As treated in this article, the docking studies and 2D-QSAR approach will pave the way for the development of new drugs while highlighting curcumin and its derivatives.

Keywords: AXL kinase, 2D-QSAR, internal and external validation, partial least square regression.

1. BACKGROUND

AXL receptor has been implicated in a number of oncogenic processes (Wu et al., 2014), AXL signaling activates many essential biological pathways for angiogenesis and metastasis, including invasion, migration, survival, cell transformation, and proliferation (Korshunov, 2012). To this date, no potent inhibitor was clearly intended for AXL, except BGB324, a small AXL inhibitor that is in clinical development sponsored by the BergenBio Company (Oien et al., 2017). BGB324 has shown that AXL inhibitor BGB324 enhances sensitivity to chemotherapy in mesothelioma and allows tumor reduction.

As mentioned earlier, developing potent and selective AXL inhibitors is always a scientists' concern. There is currently a great interest in natural compounds as potent anticancer drugs. The curcumin, is a natural polyphenol substance, isolated from the rhizome of turmeric plant *Curcuma longa* (Li et al., 2015),

The Biotechnology Lab (MedBiotech), BioInova Research center, Rabat Medical and Pharmacy School, Mohammed V University in Rabat, Rabat, Morocco.

acts on multiple targets and signaling pathways (Gupta et al., 2011). Up to now, curcumin has been shown to possess wide range of pharmacological activities, including anti-inflammatory (Ghandadi and Sahebkar, 2017), anticancer (Bar-Sela et al., 2010), osteoarthritis (Panahi et al., 2014), cardiometabolic (Mohammadi et al., 2013), depression (Esmaily et al., 2015), and respiratory (Lelli et al., 2017). These activities have been attributed to methoxy, hydroxyl, α,β-unsaturated carbonyl moiety, or diketone groups in curcumin (Aggarwal et al., 2014).

More than 40 clinical trials using curcumin were developed for the treatment of inflammatory diseases and various human cancers (Huang et al., 1988; Aoki et al., 2007; Kuttan et al., 2007). However, phase I/II clinical trials have shown that curcumin exhibits poor bioavailability in humans (Anand et al., 2007). Major reason is its low absorption causing low plasma and tissue concentration, fast metabolism, and rapid systemic elimination (Anand et al., 2007). Because of that, much work has been focused on modifications of specific functional groups of curcumin that increase its bioavailability, hence increasing its activity. These researches have been greatly facilitated by the combination of classical biochemistry tools with new approach such as the quantitative structure–activity relationship (QSAR), which have radically shortened the time and the cost needed to establish a relationship between molecular structures and their properties. Linking physicochemical properties and biological activities to the molecular structure allows, on the one hand, to explain the origin of these activities/properties and, on the other hand, to predict their activities that are unavailable (Darnag et al., 2010).

In this study, to search the molecules with enhances properties and stability, a 2D quantitative structure–activity relationship (2D-QSAR) was employed to screen out 400 molecules curcumin derivatives with the variations on carbonyl moiety and active methylene group. The QSAR model, developed by partial least square (PLS) regression (Lakhlili et al., 2016) from 128 selected AXL inhibitors, was used to analyze the inhibitory AXL activity of compounds and identify molecular properties that influence activity with a view to provide a better rational design of some more curcumin analogs in the next studies. The molecular docking studies were performed to highlight the binding mode of the most active compounds with our three-dimensional (3D) structure obtained by homology modeling (Fatima et al., 2017).

2. MATERIALS AND METHODS

2.1. Software

All the software used was open source except the molecular operating environment (MOE); the academic license used was obtained from the Chemical Computing Group ULC, 1010 Sherbooke St. West, Suite 910, Montreal, QC, Canada.

2.2. Data set selection

A total of 123 competitive ATP inhibitor molecules of AXL were selected using the canSAR3.0 (*https://cansar.icr.ac.uk)* databases on the basis of their molecular weight and the IC50. We converted the IC50 values from units of molarity (M) to pIC50 (–log IC50) to provide numerically larger data values. All molecules were randomly distributed into the training set composed of 95 molecules and the test set realized by the 28 residing molecules. The training set molecules served to build the predictive 2D-QSAR models. The test set used to assess the ability of the prediction and the extrapolation of the models obtained.

2.3. Molecular field descriptors calculation and 2D-QSAR models building

A descriptor is a quantitative property that depends on the structure of molecule. MOE software generates 184 different 2D descriptors for all training set compounds. The ''QuaSAR Contingency module,'' a statistical application in MOE, was employed systematically to select the good and potent ones. PLS regression in MOE was used to build the predictive models. PLS regression relates the descriptors as independent variables to the biological activity (pIC_{50}) of the compounds as dependent variable. The steps for model developing are as follows: (1) Constitute a database from reliable experimental measurements of the property or activity of each compound. (2) Select descriptors in relation to the activity being studied. (3) Divide this database, randomly, into a series of training set with two-third of the database and a test set constituted by the remaining one-third. (4) Establish mathematical models using the learning series. (5) Characterize the models developed by their internal validation indices and check their robustness by a randomization test (randomization) of the dependent variable Y (reply). (6) Validate the developed models using the test series

Downloaded by STOCKHOLMS UNIVERSITET from www.liebertpub.com at 04/25/19. For personal use only.

and calculate their parameters external validation statistics. (7) Develop the applicability domain of the chosen model. (8) Explore and exploit validated models to understand mechanisms and modes action.

2.4. Model validation

2.4.1. Internal validation. The ''QuaSAR fit validation'' panel application in MOE was used to realize the model validation that assesses how the model can predict the bioactivities of training set compounds accurately. This validation has been expressed by squared correlation coefficient (R^2), which compares between predicted and experimental activities. The root-mean squared error (RMSE) employed to show the error between the mean of experimental values and predicted activities. R^2 and RMSE approve if the model possesses the predictive quality reflected in the R^2.

2.4.2. Cross-validation. The ''leave-one-out'' (LOO) cross-validation test also implemented in MOE has been used to calculate the cross-validated (CV) correlation coefficient (q^2) and cross-RMSE. CV values are considered more characteristic of predictive ability of the model; many authors consider high ($q^2 > 0.5$) as an ultimate proof of the high predictive power of the QSAR model. The data utilized in obtaining q^2 are the compounds of training set used to determine R^2.

2.4.3. Z-score. The *Z*-score is another parameter of validation that represents the absolute difference between value of the model and the activity field, divided by the square root of the mean square error of data set. *Z*-score was used to detect the molecules that are outside of the adjustment say ''outliers'' (Manoj Kumar et al., 2006).

2.4.4. External validation. Test set is composed by the compounds that were not used in the model development. In several searches, the estimation of the true predictive power correlation in the developed QSAR model was done only by comparison of predicted and observed activities of an external test set (Lakhlili et al., 2016).

2.5. Curcumin-synthetic analogs library selection

A data set of 400 curcumin analogs was extracted in (.sdf) format from Curcumin Resource Database (CRDB) v.1.1 (consulted on August 25, 2017). CRDB also contains the information of various international and national patents on curcumin and its analogs. Currently the database presents the curcumin analogs with their molecular targets curated from public domain databases and published literature in peer-reviewed journals. The CRDB web portal exposes user-friendly interfaces and is expected to be highly useful to the researchers working on structure-/ligand-based molecular design of curcumin analogs.

Before predicting their activities by the developed QSAR model, ''ChemBioServer platform'' was used to analyze the compound's toxicity and search the toxic moieties based on a list of 25 known organic toxic compounds. The platform server, group of tools, was developed to facilitate computational compound screening and analysis (Athanasiadis et al., 2012). Then, we performed a filtering using Lipinski's Rule-of-Five-SCFBio (www.scfbioiitd.res. in/software) to remove compounds that do not meet the five Lipinski's Rules (Lipinski, 2004). The molecules that reside were downloaded in MOE software in (.sdf) format and that converted to (.mdb) format by the same software. These filtered molecules were screened using the best QSAR model to select those with predicted activity exceeding the threshold.

2.6. Docking studies

Molecular docking was carried out to get better insight about interaction between ligands and target. Among the 400 analogs, 63 having the predict pIC50 exceeding a threshold set (Lakhlili et al., 2016) were docked with the crystal structure of AXL kinase obtained by homology modeling approach using Auto-Dock Vina (Trott and Olson, 2010). For all ligands, Gasteiger charges were designated and the torsions, allowing to turn during the docking procedure, are added using AutoDock tools v.1.5.6 (Morris et al., 2009). The AXL receptor was prepared, polar hydrogens were assigned, the grid box was set up to provide coverage of the AXL active site, the dimensions were set at 30, 30, and 30 Å (*x*, *y*, and *z*) consisting of active site residues within the box. The receptor and ligands were saved in pdbqt format; visual inspection of the docking results and image building was done by using PyMOL software (Seeliger and de Groot, 2010).

Downloaded by STOCKHOLMS UNIVERSITET from www.liebertpub.com at 04/25/19. For personal use only.

Downloaded by STOCKHOLMS UNIVERSITET from www.liebertpub.com at 04/25/19. For personal use only.

QuaSAR_Contingency Analysis

Database : d:/cedoc ensa tanger/doctora/base de donn.
Date : Sat Jul 01 15:13:27 2017
Activity Field : pIC50
Sample Size : 96

C : Contingency Coefficient (above 0.6 is useful)
V : Cramer's V (above 0.2 is useful)
U : Entropic Uncertainty (above 0.2 is useful)
R : Linear Correlation R**2 (above 0.2 is useful)

Database fields

#	C	V	U	R	Field
1	0.60947	0.22192	0.13474	0.00087	COMPOUND_ID
2	0.95346	0.91287	1.00000	1.00000	pIC50
3	0.73891	0.23380	0.24923	0.03570	diameter
4	0.45871	0.14902	0.08971	0.00058	petitjean
5	0.45871	0.14902	0.08971	0.00246	petitjeanSC
6	0.63429	0.23685	0.17026	0.03006	radius
7	0.49284	0.16351	0.09686	0.01157	VDistEq
8	0.40743	0.12879	0.07108	0.00936	VDistMa
9	0.82780	0.42595	0.25829	0.08633	weinerPath
10	0.86692	0.18647	0.38678	0.02096	weinerPol
11	0.45743	0.14850	0.08441	0.00083	BCUT_PEOE_0
12	0.58915	0.21048	0.14191	0.02507	BCUT_PEOE_1
13	0.59498	0.21370	0.15358	0.03142	BCUT_PEOE_2
14	0.46192	0.15035	0.08722	0.00071	BCUT_PEOE_3
15	0.36066	0.11163	0.05791	0.00193	BCUT_SLOGP_0
16	0.60569	0.21974	0.13608	0.05437	BCUT_SLOGP_1
17	0.63955	0.24016	0.17188	0.01193	BCUT_SLOGP_2
18	0.41122	0.13023	0.07101	0.00001	BCUT_SLOGP_3
19	0.45743	0.14850	0.08441	0.00137	BCUT_SMR_0
20	0.68245	0.26953	0.20393	0.06805	BCUT_SMR_1
21	0.63522	0.23742	0.16981	0.01169	BCUT_SMR_2
22	0.35364	0.10914	0.04935	0.00110	BCUT_SMR_3
23	0.54368	0.18700	0.14954	0.00471	GCUT_PEOE_0
24	0.49107	0.16273	0.08997	0.00124	GCUT_PEOE_1
25	0.61161	0.22316	0.14941	0.03927	GCUT_PEOE_2
26	0.56306	0.19668	0.15390	0.00504	GCUT_PEOE_3
27	0.61781	0.22681	0.16903	0.10620	GCUT_SLOGP_0
28	0.57856	0.20477	0.14740	0.00350	GCUT_SLOGP_1
181	0.62133	0.22891	0.21591	0.03665	density
182	0.72160	0.30089	0.18244	0.02809	vdw_area
183	0.74753	0.32488	0.17644	0.00612	vdw_vol
184	0.81992	0.41345	0.25044	0.05562	logP(o/w)

Suggested Descriptors for QSAR

#	C	V	U	R	Field
1	0.78524	0.27037	0.21693	0.03719	diameter
3	0.86579	0.49946	0.36575	0.14394	BCUT_PEOE_1
4	0.86854	0.50589	0.34290	0.11019	BCUT_PEOE_2
5	0.80041	0.38545	0.22652	0.01022	BCUT_PEOE_3
7	0.86903	0.50705	0.32027	0.13012	BCUT_SMR_1
8	0.85316	0.47212	0.26935	0.12958	BCUT_SMR_2
9	0.69444	0.27860	0.21374	0.00605	GCUT_SMR_3
13	0.71385	0.29426	0.23714	0.00000	GCUT_PEOE_3
14	0.72065	0.30006	0.22134	0.00036	GCUT_SLOGP_0
15	0.64787	0.24552	0.21541	0.01518	GCUT_SLOGP_1
17	0.72784	0.30639	0.25619	0.00169	GCUT_SLOGP_3
18	0.70829	0.28965	0.21064	0.05199	GCUT_SMR_1
19	0.75468	0.33206	0.27671	0.00098	GCUT_SMR_3
20	0.78350	0.36398	0.27827	0.03969	chiral
21	0.65424	0.24972	0.18885	0.20116	reactive
23	0.85164	0.24496	0.26133	0.00012	b_heavy
36	0.78990	0.37184	0.35011	0.24663	SlogP_VSA1
37	0.78039	0.36028	0.21709	0.02499	SlogP_VSA2
38	0.66610	0.25780	0.20592	0.01739	SlogP_VSA3
40	0.64478	0.24351	0.22869	0.00116	SlogP_VSA5
42	0.79400	0.37704	0.29871	0.06923	SlogP_VSA7
43	0.76304	0.34080	0.30828	0.18563	SlogP_VSA8
44	0.75002	0.32734	0.20564	0.00449	SlogP_VSA9
46	0.67505	0.26413	0.22636	0.02173	SMR_VSA0
47	0.80001	0.38491	0.26930	0.00386	SMR_VSA1
48	0.82152	0.41593	0.28763	0.14265	SMR_VSA2
49	0.81817	0.41078	0.24712	0.05024	SMR_VSA3
50	0.82697	0.42459	0.34447	0.08785	SMR_VSA4
51	0.77015	0.34854	0.20673	0.04947	SMR_VSA5
52	0.67241	0.26225	0.22052	0.01634	SMR_VSA6

Total Time: 0.00 minutes

FIG. 1. The (2D) descriptors proposed by ''QuaSAR Contingency module'' application in MOE software. MOE, molecular operating environment.

3. RESULTS

3.1. Descriptors calculation and best model validation

Figure 1 shows the pertinent descriptors selected by ''QSAR Contingency,'' including the three main physicochemical properties hydrophobicity (SlogP_VSA, BCUT_SlogP, GCUT_SlogP), polarizability (SMR_VSA, BCUT_ SMR, GCUT_SMR), and electrostatic interactions (PEOE_VSA, BCUT_PEOE, GCUT_PEOE).

As shown in Figure 2, the PLS regression in conjugation with leave one out (LOO) CV techniques implemented in ''QuaSAR-Model'' module in MOE was used to develop the 2D-QSAR models through the PLS of the training set (95 compounds). The statistical fitness of the best QSAR model was expressed by means of various statistical parameters such as a correlation coefficient (R^2) of 0.99 and an RMSE of 0.560.

The plot in the Figure 3 presents the relationship between observed and predicted values from the training and test set. The predictive performance on validation confirmed by the CV RMSE of 0.672 and CV correlation coefficient of $q^2 = 0.707$.

Any compound with a *Z*-score value >2.5 was considered as an outlier (Manoj Kumar et al., 2006). Thus, in external validation, the test set compounds were used to evaluate the predictive ability of the best model. The test set molecules are displayed in Table 1 that shows the difference between experimental (pIC50) versus predicted activity ($PRED) in this data is <1.

3.2. Curcumin-synthetic analogs library screening

We threaded 400 compounds extracted from CRDB using Lipinski's Rule-of-Five in the FILTER program; then, we analyzed their toxicity. Their activity was predicted by ''Model evaluate'' procedure in

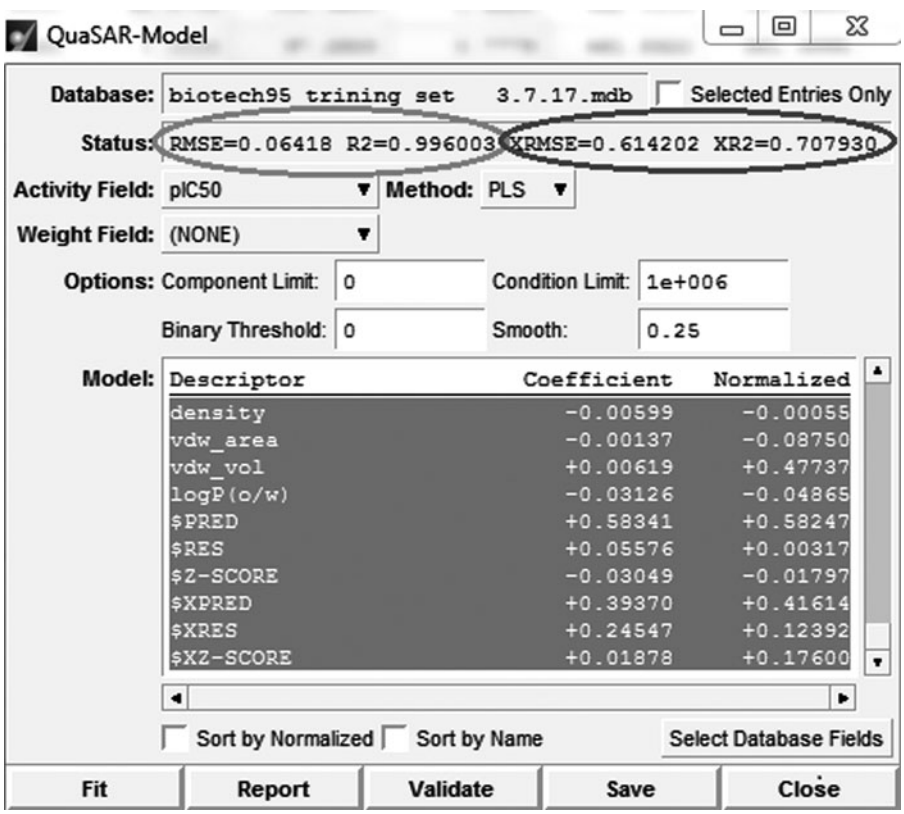

FIG. 2. Fitting the dependent variable (pIC50) to the independent variables (descriptors) of the training set in the MOE ''QuasSAR-Model'' to generate the quantitative structure–activity relationship model and the parameters of validation. Note that the gray circle surrounds the validation parameters (R2 and RMSE), whereas the black circle surrounds the cross-validation parameters. RMSE, root-mean squared error.

Downloaded by STOCKHOLMS UNIVERSITET from www.liebertpub.com at 04/25/19. For personal use only.

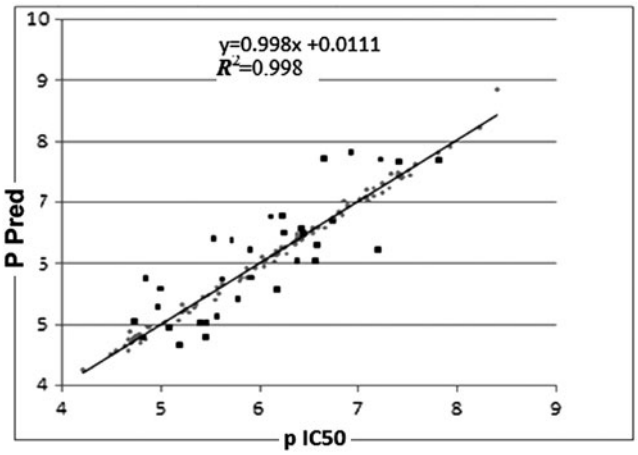

FIG. 3. Plot of predicted pIC50 values versus experimental ones for the PLS model. Note the compound of training set in dots and prediction set in dots. PLS, partial least square.

MOE. Only 63 molecules with a pIC50 > 6, considered a threshold (Lakhlili et al., 2016), were prepared and docked into pocket site of AXL tyrosine kinase structure using AutoDock Vina.

3.3. Molecular docking results

The docking scores (affinity) were set between −9.0 and −3.4 kcal/mol; the compounds with the low energy conformations and the best predicted activities were selected to analyze and evaluate their interaction with the AXL active site. Molecular docking studies revealed that the CID10765707, CID11257493, and CID21159180 compounds have a low binding energy −9.0, −8.6, and −8.2 kcal/mol, respectively, and the best predicted activities. They are used further to study their interaction mode with the target protein. At a distance of 4 Å, the active site encompasses 45 amino acids (Messoussi et al., 2014), the most relevant are Leu600 serving as gatekeeper and the triplet Pro 621, Phe 622, and Met623 forming a hinge, Lys 567 (the binding site key residue of ATP), Asp 690, Phe 691, and Gly 692 (the DFG-motif in activation loop) (Fatima et al., 2017).

Figure 4 shows that the three compounds interact with the residues around the catalytic site by hydrogen and hydrophobic bonds. Hζ-atom of the Met 623 in the hinge interacts by H bonding with hydroxyl group in phenyl rings oriented in the deep hydrophobic pocket of the three compounds. On the other side, the second hydroxyl phenyl-end exposed to the open gate elaborates the three H bonding with CID10765707 and CID21159180 compounds: the first H bonding with Ala 689 of the activation loop, the second H bonding with Asp 690 one residue of DFG motif in the activation loop, and the third with Lys 567 positioned on a β-sheet of N-lobe (Fatima et al., 2017). The CID21159180 exhibits two other hydrogen bonds with Glu585 and Asp627. As for the CID11257493 compound, the same hydroxyl phenyl-end creates hydrogen bonds with Asp672, Arg676, and Asn677. Several hydrophobic interactions were also observed with Glu544, Glu546, Lys624, and Asp690. The three curcumin synthetic analogs showed a higher affinity to AXL receptor identical to that of curcumin and its natural derivatives (Fatima et al., 2017). The CID 21159180 compound expressed a better predicted activity value reported in Table 2 that includes the 2D structures of three inhibitors (extracted from NCBI-PubChem) and these molecular properties, predicted activities, binding affinity, and key residues that interact with protein target.

4. DISCUSSION

In this study, a detailed 2D-QSAR was developed on a series of curcumin synthetic derivatives with methoxy, hydroxyl, α,β-unsaturated β-diketone moiety modifications to detect if they possess an anticancer activity against AXL kinase. Only 2D descriptors generated by ''QSAR Contingency'' application in MOE were selected to develop the QSAR models by PLS regression; the best one has an acceptable statistical quality and predictive potential as indicated by the value of cross-validated squared correlation coefficient ($q^2 = 0.707$) and the results of the external validation. The ligands library screening was done on 400 curcumin analogs. All ligands were filtered by ChemBioServer platform to remove the compounds that do

Downloaded by STOCKHOLMS UNIVERSITET from www.liebertpub.com at 04/25/19. For personal use only.

Downloaded by STOCKHOLMS UNIVERSITET from www.liebertpub.com at 04/25/19. For personal use only.

Table 1. The External Validation Results for the Predictive Model Generated by Molecular Operating Environment Software

	Molecule	*COMPOUND_ID*	*Keywords*	*pIC50*	*$pred*	*Result_1*
1	OC1CC(Nc2nc(ncc2c2ncccc2)NCCCC)C1	1169928	3-{[2-(Butylamino)-5-(pyridin-2-yl) pyrimidin-4-yl]amino}cyclobutan-1-ol	5.5544	4.7398	0.8146
2	OC1CCC (Nc2nc(ncc2C(=O)NCc2ccc(	1173180	2-(Butylamino)-4-[(4-hydroxycyclohexyl) amino]-N-{[4-(1H-imidazol-1-yl) phenyl]methyl}pyrimidine-5-carboxamide	6.4437	6.9751	–0.5314
3	OC1CCC(Nc2nc(ncc2-c2ncc(cc2)C(=O) NC2CCN(CC2)C)NCCCC)CC1	1173654	6-[2-(Butylamino)-4-[(4-hydroxycyclohexyl) amino]pyrimidin-5-yl]-N-(1-methylpiperidin-4-yl)pyridine-3-carboxamide	7.2147	7.5525	–0.3378
4	OC1CCC(Nc2nc(ncc2-c2ncc(cc2)C(=O)	1173818	4-{[2-(Pentylamino)-5-(pyridin-yl)pyrimidin-4-yl] amino cyclohexan-1-ol	6.1871	5.7164	0.4706
5	Fc1ccc(NC(=O)c2cnc(nc2NCC2CCC(	1173982	4-{[(4-Aminocyclohexyl)methyl amino}-2-(butylamino)	5.6990	6.3974	–0.6985
6	O1C(OC)c2c(c(O)c(O)c(O)c2C)C1=O	1175090	5,6,7-Trihydroxy-3-methoxy 4-methyl-1, 3-dihydro-2-	5.1945	4.6892	0.5053
7	OC1CCC(Nc2nc(ncc2C(=O)NCCCC) NCCCC)CC1	1175493	N-butyl-2-(butylamino)-4-[(4hydroxycyclohexyl) amino]	5.5229	6.1573	–0.6344
8	OCCCNc1nc(ncc1-c1ncccc1)NCCCC	1176518	3-{[2-(Butylamino)-5-(pyridin-2-yl)pyrimidin-4-yl]amino}cyclohexan-1-ol, 1173818	5.0048	5.2211	–0.2163
9	o1c2c(cc1-c1c(C=O)c(O)c(O)c(O)c1C) c(C=O)c(C)c(O)c2O	1181146	2-(2-Formyl-3,4,5-trihydroxy-6-methylphenyl)6,7-dihydroxy-5-methyl-1-	6.6576	8.0066	–1.3491
10	OC1CCC(Nc2nc(ncc2-c2ncccc2)NC)CC1	1182355	4-{[2-(Methylamino)-5-(pyridin-2-yl)pyrimidin-4-yl]amino}	5.4067	4.8502	0.5565
11	OC1CCC(Nc2nc(ncc2-c2ncc(cc2) CNC2CCCCC2)NCCCC)CC1	1183423	4-{[2-(Butylamino)-5-{5-[(cyclohexylamino)	7.4202	7.6699	–0.2497
12	Fc1ccc(cc1)CNC(=O)c1cnc (nc1NC1CCC(O)CC1)NCCCC	1184420	2-(Butylamino)-N-[(4-fluorophenyl)methyl4-[(4-hydroxycyclohexyl)amino	6.1024	6.5987	–0.4963
13	O1CCN(CC1)Cc1ccc(nc1)-c1cnc (nc1NC1CCC(O)CC1)NCCCC	1185438	4-{[2-(Butylamino)-5-[5-(morpholin lmethyl) pyridin-2-yl]pyrimidin-4yl]amino} cyclohexan-1-ol, 1185438	6.5686	5.7785	0.7902
14	O(C)c1cc(NC(=O)c2cnc(nc2NC2 CCC(O)CC2)NCCCC)ccc1	1185778	2-(Butylamino)-4-[(4hydroxycyclohexyl) amino]-N-(3-methoxyphenyl)pyrimidine-5-carboxamide,	5.7696	5.5122	0.2574
15	OC1CCC(Nc2nc(ncc2-c2ncccc2) NC(CCC)C)CC1	1186289	4-{[2-(Pentan-2-ylamino)-5-(pyridin-2-yl) pyrimidin-4-yl]amino}cyclohexan-1-ol,	5.0947	5.1488	–0.0541

(*continued*)

Downloaded by STOCKHOLMS UNIVERSITET from www.liebertpub.com at 04/25/19. For personal use only.

Table 1. (Continued)

	Molecule	*COMPOUND_ID*	*Keywords*	*pIC50*	*$pred*	*Result_1*
16	o1c2c(nc1C)cc(OC)c(O)c2C[C]1([CH]2CCC=C(C)[C]2(CC[CH]1C)C)C	1186756	7-{[(1R,2S,4aR,8aS)-1,2,4a,5-tetramethyl1,2,3,4,4a,7,8,8aoctahydronaphthalen-1-yl] methyl}-5-methoxy-2-methyl-1,3-benzoxazol-6-ol	4.8327	6.4054	–1.5727
17	OC1CCC(Nc2nc(ncc2-c2ncccc2)NCC)CC1	1187876	4-{[2-(Ethylamino)-5-(pyridin-2-yl)pyrimidin-4-yl] amino}cyclohexan-1-ol	5.4522	4.8624	0.5898
18	OC1CCC(Nc2nc(ncc2-c2ncccc2)NCCCO)CC1	1190299	4-({2-[(3-Hydroxypropyl)amino]-5-(pyridin-2-yl)pyrimidin-4-yl}amino)cyclohexan-1-ol,1190299	4.8239	4.5377	0.2862
19	OC1CCC(Nc2nc(ncc2-c2ncccc2)NCCCCO)CC1	1190334	4-({2-[(4-Hydroxybutyl)amino]-5-(pyridin-2-yl)pyrimidin-4-yl}amino)cyclohexan-1-ol	5.4609	4.8147	0.6462
20	OC1CCC(Nc2nc(ncc2-c2ncccc2)NCCc2ccccc2)CC1	1192573	4-({2-[(2-Phenylethyl)amino]-5-(pyridin-2-yl)pyrimidin-4-yl}amino)cyclohexan-1-ol,	6.3665	6.2013	0.1653
21	O1CCC(NC(=O)c2cnc(nc2NC2CCC(O)CC2)NCCCC)CC1	1193564	2-(Butylamino)-4-[(4hydroxycyclohexyl)amino]-N-(oxan-4-yl)pyrimidine-5-carboxamide,	6.2366	6.4356	–0.1990
22	n1c(NCC2CCNCC2)c(cnc1NCCCC)-c1ncccc1	1194959	2-N-butyl-4-N-(piperidin-4-ylmethyl)-5-(pyridin-2-yl)pyrimidine-2,4-diamine,	5.8928	6.5252	–0.6324
23	OC1CCC(Nc2nc(ncc2-c2ncccc2)NCCO)CC1	1195433	4-({2-[(2-Hydroxyethyl)amino]-5-(pyridin-2-yl)pyrimidin-4-yl}amino)cyclohexan-1-ol,	4.7328	4.7602	–0.0273
24	n1c(NC2CCC(CC2)CN)c(cnc1NCCCC)-c1ncccc1	1195846	4-N-[4-(Aminomethyl)cyclohexyl]-2-N-butyl-5-(pyridin-2-yl)pyrimidine-2,4-diamine,	6.7447	6.7404	0.0043
25	OC1CCC(Nc2nc(ncc2C(=O)NC2CCN(CC2)c2ncccn2)NCCCC)CC1	1196013	2-(Butylamino)-4-[(4hydroxycyclohexyl) amino]-N-[1-(pyrimidin-2-yl)piperidin-4-yl]pyrimidine-5-carboxamide, 1196013	6.2518	6.9331	–0.6813
26	OC1CCC(Nc2nc(ncc2c2ncc(cc2)CN2CCN(CC2)C)NCCCC)CC1	1196148	4-{[2-(Butylamino)-5-{5-[(4-methylpiperazin-1-yl)methyl]pyridin-2-yl}pyrimidin-4yl]amino}cyclo hexan-1-ol,	6.5850	6.0420	0.5430
27	OC1CCC(Nc2nc(ncc2C(=O)NC2CCCCC2)NCCCC)CC1	1197346	2-(Butylamino)-N-cyclohexyl-4-[(4hydroxy cyclohexyl)amino]pyrimidine-5carboxa mide, 1197346	6.4318	6.4972	–0.0654
28	S(=O)(=O)(N1CCOCC1)c1ccc(NC(=O)c2cnc(nc2NC2CCC(O)CC2)NC)cc1	1199153	4-[(4-Hydroxycyclohexyl)amino]-2-(methyl amino)-N-[4-(morpholine-4sulfonyl)phenyl] pyrimidine-5-carboxamide,	5.9208	6.1764	–0.2556

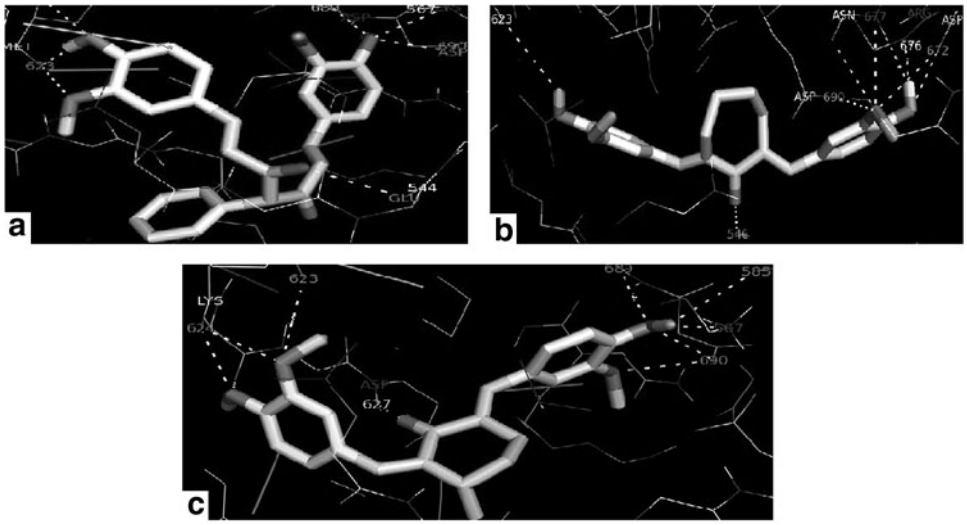

FIG. 4. **(a)** All interactions of CID 10765707 against AXL protein. **(b)** All interactions of CID 11257493 against AXL protein. **(c)** All interactions of CID 21159180 against AXL protein.

not meet the Lipinski's Rule-of-Five and having a high toxicity effect. A total of 355 compounds resulting will be used to predict their activities by the developed QSAR model; only 63 with pIC50 ≥ 6 have been selected to test their interaction with AXL kinase by molecular docking.

The docking scores (affinity) were situated between −9.0 and −3.4 kcal/mol. QSAR analyses revealed that the three compounds CID10765707, CID11257493, and CID21159180 exhibit the best predicted

Table 2. Compounds 2D Structure and Molecular Properties, Predicted Activities, Binding Affinity, and the Key Residues That Interact with AXL Kinase

Compound 2D structure	*Molecular weight (g/mol)*	*Log P*	*Predicted activity*	*Binding affinity, kcal/mol*	*Interactions of amino acid residues*
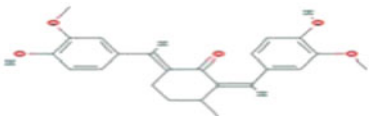 **CID21159180:** (2Z,6E)-2,6-bis [(4-hydroxy-3-methoxy phenyl) methylidene]-3-methylcyclohexan-1-one	380.0	4.581	6.15	−9.0	**Met** 623; **Asp 627**; Lys624; **Lys**567; **Ala 689**; **Asp**690; **Asp**690; Glu585
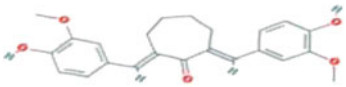 **CID11257493:** (2E,7E)-2,7-bis [(4-hydroxy 3methoxyphenyl) methylidene]cycloheptan 1-one	380.0	4.725	7.39	−8.6	**Met** 623; **Asp**672 **Arg**676; **Glu**546; **Asn677**; **Asp**690
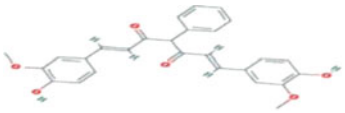 **CID10765707:** (1E,6E)-1,7-bis (4-hydroxy-3-methoxyphenyl)-4-phenylhepta-1,6-diene-3,5-dione	444.0	4.763	11.31	−8.2	**Met 623; Lys567 Ala689; Asp690 Glu544**

The three ID compounds and the most important residues are shown in boldface.

Downloaded by STOCKHOLMS UNIVERSITET from www.liebertpub.com at 04/25/19. For personal use only.

activity with high affinity to AXL kinase. They are characterized by their symmetric structures with two hydroxyl groups (OH) at C-4′ and two ortho-methoxy groups (OCH3) at C-3′ in bilateral phenyl rings. The three analogs were designed with the same substitution on α,β-unsaturated β-diketone moiety. In compounds CID11257493 and CID21159180, the β-diketone moiety is removed and replaced by a cyclic ketone, a cycloheptanone is linked to α,β-unsaturated fragment in CID11257493, whereas the second compound a methyl-cyclohexanone group is attached to the same fragment (compound's structure exposed in Table 1). Concerning CID10765707 compound, a phenyl-heptadiene was planted on β-diketone moiety.

In this study, a hydroxyl group attached to the aromatic rings was imperative to enhance the activity of curcumin analogs by building many hydrogen bonds around the active site, either at the hinge or at the activation loop. These results are similar to Leong et al. (2015) study who showed, in structure–activity comparison, that dihydroxylphenyl ring is crucial for analog's bioactivities. Chen et al. indicate that a hydroxyl group removal or substitution resulted in a reduction of analog's activity and low affinity (Ji and Shen, 2009; Chen et al., 2014). Moreover, we noticed that the activity of three analogs is obtained when the phenolic hydroxyl group is present with two methoxy groups of each ring. Also the number of methoxy groups in the each phenyl rang as well as their position was important for phenyl radical stability (Barclay et al., 2000; Chandru et al., 2007); loss of one or two methoxy groups reduced the analog effect (Cocorocchio et al., 2018).

In another side, the high affinity of these three compounds to AXL kinase may be due to the structure modification of a β-diketone moiety since, it has been suggested that diketone fragment of curcumin is not indispensable for the analog activity (Simoni et al., 2008). Selvam et al. (2005) showed that the structure modification of the β-diketone fragment increases the inhibitory effects of curcumin against COX-2 protein. In the same way, deleting β- diketone of curcumin may increase the stability and antiproliferative activity.

Furthermore, Xu et al. (2013) have deduced in their study that a novel α,β-unsaturated cyclohexanone analogs designed through altering its β-diketones exhibit potent antiproliferative activity against EGFR by suppressing levels of protein in two human tumor cell lines. Liang et al. (2009) mentioned that the reactive β-diketone moiety is responsible for the pharmacokinetic limitation of curcumin. It contributes to the instability of curcumin under physiological conditions, poor absorption, and fast metabolism. They designed a cyclopentanone and cyclohexanone analog without β-diketone; their results showed that the stability of these analogs tested in vitro was greatly enhanced and their pharmacokinetic studies realized in vivo were also significantly improved (Liang et al., 2009). On the basis of these findings, it is clear that hydroxyl and methoxy groups implanted in the each phenolic group are essential for the activity. Besides, it has also been found that the removing of β-diketone moiety and its replacement by a cyclic ketone enhances the activity.

CONCLUSION

In this study, The QSAR approach combined with molecular docking studies have revealed that the compounds CID10765707, CID11257493, and CID21159180, which bear dihydroxy dimethoxyphenoxyl groups and the major modification in α,β-unsaturated β-diketone moiety portion exhibited significantly higher activity and the best affinity against AXL kinase. The three selected compounds will undergo in vitro and in vivo analyses to better understand their physicochemical and structural characteristics associated with their biological properties, which will help further to design novel AXL inhibitors in completion with ATP more stable than curcumin with high potent activity and better bioavailability.

ACKNOWLEDGMENTS

This study was carried out under national funding from the Moroccan Ministry of Higher Education and Scientific Research (PPR Program) to A.I. This study was also supported by a grant from the NIH for H3Africa BioNet to A.I. and Institute of Research of Lalla Salma Foundation.

AUTHOR DISCLOSURE STATEMENT

The authors declare there are no competing financial interests.

Downloaded by STOCKHOLMS UNIVERSITET from www.liebertpub.com at 04/25/19. For personal use only.

REFERENCES

Aggarwal, B.B., Deb, L., and Prasad, S. 2014. Curcumin differs from tetrahydrocurcumin for molecular targets, signaling pathways and cellular responses. *Mol. Basel Switz.* 20, 185–205.

Anand, P., Kunnumakkara, A.B., Newman, R.A., et al. 2007. Bioavailability of curcumin: Problems and promises. *Mol. Pharm.* 4, 807–818.

Aoki, H., Takada, Y., Kondo, S., et al. 2007. Evidence that curcumin suppresses the growth of malignant gliomas in vitro and in vivo through induction of autophagy: Role of Akt and extracellular signal-regulated kinase signaling pathways. *Mol. Pharmacol.* 72, 29–39.

Athanasiadis, E., Cournia, Z., and Spyrou, G. 2012. ChemBioServer: A web-based pipeline for filtering, clustering and visualization of chemical compounds used in drug discovery. *Bioinforma. Oxf. Engl.* 28, 3002–3003.

Barclay, L.R., Vinqvist, M.R., Mukai, K., et al. 2000. On the antioxidant mechanism of curcumin: Classical methods are needed to determine antioxidant mechanism and activity. *Org. Lett.* 2, 2841–2843.

Bar-Sela, G., Epelbaum, R., and Schaffer, M. 2010. Curcumin as an anti-cancer agent: Review of the gap between basic and clinical applications. *Curr. Med. Chem.* 17, 190–197.

Chandru, H., Sharada, A.C., Bettadaiah, B.K., et al. 2007. In vivo growth inhibitory and anti-angiogenic effects of synthetic novel dienone cyclopropoxy curcumin analogs on mouse Ehrlich ascites tumor. *Bioorg. Med. Chem.* 15, 7696–7703.

Chen, B., Zhu, Z., Chen, M., et al. 2014. Three-dimensional quantitative structure–activity relationship study on antioxidant capacity of curcumin analogues. *J. Mol. Struct.* 1061, 134–139.

Cocorocchio, M., Baldwin, A.J., Stewart, B., et al. 2018. Curcumin and derivatives function through protein phosphatase 2A and presenilin orthologues in *Dictyostelium discoideum*. *Dis. Model. Mech.* 11.

Darnag, R., Mostapha Mazouz, E.L., Schmitzer, A., et al. 2010. Support vector machines: Development of QSAR models for predicting anti-HIV-1 activity of TIBO derivatives. *Eur. J. Med. Chem.* 45, 1590–1597.

Esmaily, H., Sahebkar, A., Iranshahi, M., et al. 2015. An investigation of the effects of curcumin on anxiety and depression in obese individuals: A randomized controlled trial. *Chin. J. Integr. Med.* 21, 332–338.

Fatima, G., Loubna, A., Lakhlili, W., et al. 2017. In silico inhibition studies of AXL kinase by curcumin and its natural derivatives. *J. Appl. Bioinforma. Comput. Biol.* 06. https://doi.org/10.4172/2329-9533.1000142

Ghandadi, M., and Sahebkar, A. 2017. Curcumin: An effective inhibitor of interleukin-6. *Curr. Pharm. Des.* 23, 921–931.

Gupta, S.C., Prasad, S., Kim, J.H., et al. 2011. Multitargeting by curcumin as revealed by molecular interaction studies. *Nat. Prod. Rep.* 28, 1937–1955.

Huang, M.T., Smart, R.C., Wong, C.Q., et al. 1988. Inhibitory effect of curcumin, chlorogenic acid, caffeic acid, and ferulic acid on tumor promotion in mouse skin by 12-O-tetradecanoylphorbol-13-acetate. *Cancer Res.* 48, 5941–5946.

Ji, H.-F., and Shen, L. 2009. Interactions of curcumin with the PfATP6 model and the implications for its antimalarial mechanism. *Bioorg. Med. Chem. Lett.* 19, 2453–2455.

Korshunov, V.A. 2012. Axl-dependent signaling: A clinical update. *Clin. Sci. Lond. Engl.* 1979 122, 361–368.

Kuttan, G., Kumar, K.B.H., Guruvayoorappan, C., et al. 2007. Antitumor, anti-invasion, and antimetastatic effects of curcumin. *Adv. Exp. Med. Biol.* 595, 173–184.

Lakhlili, W., Yasri, A., and Ibrahimi, A. 2016. Structure–activity relationships study of mTOR kinase inhibition using QSAR and structure-based drug design approaches. *Onco Targets Ther.* 9, 7345–7353.

Lelli, D., Sahebkar, A., Johnston, T.P., et al. 2017. Curcumin use in pulmonary diseases: State of the art and future perspectives. *Pharmacol. Res.* 115, 133–148.

Leong, S.W., Mohd Faudzi, S.M., Abas, F., et al. 2015. Nitric oxide inhibitory activity and antioxidant evaluations of 2-benzoyl-6-benzylidenecyclohexanone analogs, a novel series of curcuminoid and diarylpentanoid derivatives. *Bioorg. Med. Chem. Lett.* 25, 3330–3337.

Li, C.-P., Li, J.-H., He, S.-Y., et al. 2015. Effect of curcumin on p38MAPK expression in DSS-induced murine ulcerative colitis. *Genet. Mol. Res. GMR* 14, 3450–3458.

Liang, G., Shao, L., Wang, Y., et al. 2009. Exploration and synthesis of curcumin analogues with improved structural stability both in vitro and in vivo as cytotoxic agents. *Bioorg. Med. Chem.* 17, 2623–2631.

Lipinski, C.A. 2004. Lead- and drug-like compounds: The rule-of-five revolution. *Drug Discov. Today Technol.* 1, 337–341.

Manoj Kumar, P., Karthikeyan, C., Hari Narayana Moorthy, N.S., et al. 2006. Quantitative structure-activity relationships of selective antagonists of glucagon receptor using QuaSAR descriptors. *Chem. Pharm. Bull. (Tokyo)* 54, 1586–1591.

Messoussi, A., Peyronnet, L., Feneyrolles, C., et al. 2014. Structural elucidation of the DFG- Asp in and DFG-Asp out states of TAM kinases and insight into the selectivity of their inhibitors. *Mol. Basel Switz.* 19, 16223–16239.

Downloaded by STOCKHOLMS UNIVERSITET from www.liebertpub.com at 04/25/19. For personal use only.

Mohammadi, A., Sahebkar, A., Iranshahi, M., et al. 2013. Effects of supplementation with curcuminoids on dyslipidemia in obese patients: A randomized crossover trial. *Phytother. Res. PTR* 27, 374–379.

Morris, G.M., Huey, R., Lindstrom, W., et al. 2009. AutoDock4 and AutoDockTools4: automated docking with selective receptor flexibility. *J. Comput. Chem.* 30, 2785–2791.

Oien, D.B., Garay, T., Eckstein, S., et al. 2017. Cisplatin and pemetrexed activate AXL and AXL inhibitor BGB324 enhances mesothelioma cell death from chemotherapy. *Front. Pharmacol.* 8, 970.

Panahi, Y., Rahimnia, A.-R., Sharafi, M., et al. 2014. Curcuminoid treatment for knee osteoarthritis: A randomized double-blind placebo-controlled trial. *Phytother. Res. PTR* 28, 1625–1631.

Seeliger, D., and de Groot, B.L. 2010. Ligand docking and binding site analysis with PyMOL and Autodock/Vina. *J. Comput. Aided Mol. Des.* 24, 417–422.

Selvam, C., Jachak, S.M., Thilagavathi, R. et al. 2005. Design, synthesis, biological evaluation and molecular docking of curcumin analogues as antioxidant cyclooxygenase inhibitory and anti-inflammatory agents. *Bioorg. Med. Chem. Lett.* 15, 1793–1797.

Simoni, D., Rizzi, M., Rondanin, R. et al. 2008. Antitumor effects of curcumin and structurally beta-diketone modified analogs on multidrug resistant cancer cells. Bioorg. *Med. Chem. Lett.* 18, 845–849.

Trott, O., and Olson, A.J. 2010. AutoDock Vina: Improving the speed and accuracy of docking with a new scoring function, efficient optimization and multithreading. *J. Comput. Chem.* 31, 455–461.

Wu, X., Liu, X., Koul, S., et al. 2014. AXL kinase as a novel target for cancer therapy. *Oncotarget* 5, 9546–9563.

Xu, Y.-Y., Cao, Y., Ma, H., et al. 2013. Design, synthesis and molecular docking of α,β-unsaturated cyclohexanone analogous of curcumin as potent EGFR inhibitors with antiproliferative activity. *Bioorg. Med. Chem.* 21, 388–394.

Address correspondence to:
Fatima Ghrifi, PhD Student
The Biotechnology Lab (MedBiotech)
BioInova Research center
Rabat Medical and Pharmacy School
Mohammed V University in Rabat
Avenue Mr belarbi Alaoui
Suissi-Rabat
BP6203 Rabat Institutes
Rabat 10000
Morocco

E-mail: ghrifatima1000@gmail.com

Downloaded by STOCKHOLMS UNIVERSITET from www.liebertpub.com at 04/25/19. For personal use only.